European Archives of Oto-Rhino-Laryngology (2024) 281:3423–3430
https://doi.org/10.1007/s00405-023-08418-7

OTOLOGY

Evaluation of subarcuate canal on CT images in the perspective of clinical basis

Davut Akduman[1] · Hilal Melis Altıntaş[2] · Berin Tuğtağ Demir[2] · Ali Köksal[3] · Fatih Çankal[4] · Dilara Patat[2] · Burak Bilecenoğlu[2]

Received: 2 October 2023 / Accepted: 12 December 2023 / Published online: 2 January 2024

Abstract

Objectives The aim of our study to contribute to the field of morphometrics by including measurements of the SAC and SAF and their distances from surrounding structures, particularly for surgeons involved in retrosigmoid approach for internal acoustic meatus tumor surgery and cerebellopontine angle surgery. Although there is limited information in the literature regarding the role of the subarcuate fossa (SAF) and subarcuate canal (SAC), it has been suggested that the SAC may be a potential pathway for infection from the middle ear to the posterior cranial fossa, and cerebellar abscesses may have this origin.

Methods For the images of our study, computerized tomography images of 118 individuals (59 females and 59 males) between the ages of 18–65 who applied to Bayındır Health Group.

Results The width of the cranial opening of the subarcuate canal was determined as 44 ± 0.54 mm, width of the labyrinth opening of the subarcuate canal was determined as 60 ± 0.42 mm, Length of the subarcuate canal was determined as 8.79 ± 2.31 mm, width of the subarcuate canal was determined as 5.54 ± 1.75 mm, and depth of subarcuate fossa was determined as 1.67 ± 0.69 mm. The distance of the cranial opening of the subarcuate canal to the superior semicircular canal (SSC–SAC/C) was measured as 5.33 ± 1.81 mm, The distance of the labyrinth opening of the subarcuate canal to the superior semicircular canal (SSC–SAC/L) was measured as $3.90 \pm .98$ mm, length of the petrous part of the temporal bone medial to the anterior semicircular canal measured from the apex to the SSCD (PLM) was measured as 33.56 ± 0.42 mm. No statistically significant differences were found between the right and left sides.

Conclusions The morphometric measurements obtained in this study can provide useful information for neurosurgeons, neurotologist and otolaryngologists involved in retrosigmoid approach for internal acoustic meatus tumor surgery and cerebellopontine angle surgery, and for patients undergoing cochlear implant planning with a retrofacial approach.

Keywords Subarcuate canal · Subarcuate fossa · Computed tomography · Internal acoustic meatus

✉ Davut Akduman
dr.akduman@gmail.com

Hilal Melis Altıntaş
hilalmelisaltintas@gmail.com

Berin Tuğtağ Demir
berin.tugtag@ankaramedilpol.edu.tr

Ali Köksal
akoksal@bayindirhastanesi.com.tr

Fatih Çankal
fcankal@yahoo.com

Dilara Patat
dilara.patat@ankaramedilpol.edu.tr

Burak Bilecenoğlu
burak.bilecenoglu@ankaramedilpol.edu.tr

[1] Ankara Atatürk Sanatoryum Training and Research Hospital, Gulhane Faculty of Medicine, Department of Otorhinolaryngology, University of Health Science Turkey, Ankara, Turkey

[2] Faculty of Medicine, Department of Anatomy, Ankara Medipol University, Ankara, Turkey

[3] Department of Radiology, Bayındır Hospital Söğütözü, Ankara, Turkey

[4] Department of Radiology, Pursaklar State Hospital, Ankara, Turkey

Introduction

Temporal bone containing nerves, arteries, veins, cochlea and vestibular organs has a complex anatomy. Accessing to the internal acoustic canal, petrous apex, labyrinth, facial nerve, middle ear and cerebellopontin angle requires drilling through varying densities of bone. The limited visibility of the surgical field and narrow surgical corridors may be subject to accidental damage to anatomical structures that need to be protected [1]. For example, internal acoustic meatus tumor, cerebellopontine angle tumor and semicircular canal injury can lead to severe sensorineural hearing loss, accidental injury to the middle ear ossicles can cause conductive hearing loss, permanent changes in taste may occur due to chorda tympani damage, accidental damage to the facial nerve carries risk for facial paralysis or penetration of the surrounding dura may cause cerebrospinal fluid leakage [1]. The radiological anatomy of the temporal bone has been extensively studied in the literature, but little information has been reported regarding the subarcuate canal (SAC), also known as the petromastoid canal or Chatellier's antrocerebellar canal. SAC, which is wider and more voluminous in infants and young children, either becomes invisible or becomes a barely perceptible radiolucent line in adults [2]. The SAC is a structure that originates from the subarcuate fossa (SAF) and connects the mastoid antrum to the posterior cranial fossa [3–9]. The lateral opening of the SAC is usually located in the antrum or periantral mastoid cells, and bends slightly forward before opening to the periantral mastoid cells [3, 10]. The subarcuate artery (SAA) originating from the anterior inferior cerebellar artery (AICA) or labyrinthine artery, which supplies the otic capsule of the semicircular canals, part of the vestibule, facial canal, and mucosa of the mastoid cells, passes through the SAC. In addition, the subarcuate vein, which drains into the superior petrosal sinus or directly into the sigmoid sinus along with the extension of the dura mater, also passes through the SAC [6–8]. As the size of the SAC decreases with age, the vascular structures that pass through it become vulnerable to injury and damage during surgical procedures [9].

The SAF is a shallow depression that starts from the medial opening of the SAC, located on the posterior surface of the petrous part of the temporal bone, below the arch of the superior semicircular canal (SSC), and superolateral to the internal acoustic meatus [11]. The SAF is covered by the dura mater and is an important anatomical structure to consider during retrosigmoid surgical approaches. Injury to the dura mater covering the SAF can cause bleeding by damaging the SAA in the region, leading to many middle ear problems, such as infections and vertigo [12, 13]. SAC trauma can also cause disturbing bleeding as well as cerebrospinal fluid leakage and facial nerve injury [11, 14, 15]. The anatomical position of the bony labyrinth is important in translabyrinthine approaches used in intralabyrinthine or internal acoustic meatus (IAM) lesions to transfer the drainage of the petrous region to the mastoid region. Therefore, in surgical procedures requiring intervention in the bony labyrinth, the SAC–SSC relationship should be determined well, because the SAC passes under the arch of the SSC and is located between the two openings of the canal [16].

Although there is limited information in the literature regarding the role of the SAF and SAC, it has been suggested that the SAC may be a potential pathway for infection from the middle ear to the posterior cranial fossa, and that 3.2% of cerebellar abscesses may have this origin [5–17, 17–19]. Despite its clinical importance, the small size of the SAC and its course through the SSC create a serious obstacle to visualizing its structure and location on radiographs, and thus it has rarely been the subject of morphological studies [9, 15, 18]. In fact, knowledge of the anatomy and radiologic appearance of the subarcuate region is essential for recognizing temporal bone fracture lines in cases of head trauma, or for more accurately visualizing the bony components within the petrous bone [3, 5, 11, 19] Particularly as a potential complication of cerebellopontine angle surgery, knowledge of the region is critical for diagnosing cerebrospinal fluid fistulas that may arise from the SAF [6–11, 14, 15, 17, 19]. Undesirable damage and complications related to SAA can be prevented by preoperative planning using CT-based measurements, which can also benefit from the findings of this study [20, 21]. Therefore, investigating the morphological features of the SAC and examining its topography using CT will be a useful guide for surgeons during interventions. In this regard, our study aims to contribute to the field of morphometrics by including measurements of the SAC and SAF and their distances from surrounding structures, neurosurgeons, neurotologist and otolaryngologists involved in retrosigmoid approach for internal acoustic meatus tumor surgery and cerebellopontine angle surgery, and for patients undergoing cochlear implant planning with a retrofacial approach..

Methods

Ethics

This study was performed in line with the principles of the Declaration of Helsinki. Approval was granted by the Ethics Committee of Bayındır Hospital (Date 25.04.2023—No 11/23). All study subjects had signed the Patient Informed Consent (PIC) prior to imaging.

Research design

For the images of our study, computerized tomography (CT) images of 118 individuals (59 females and 59 males) between the ages of 18–65 who applied to Bayındır Health Group Hospital for any reason and had no pathological findings, available in the archives, were used.

The inclusion and exclusion criteria for the study were determined as follows:

Inclusion criteria

- Patients between the ages of 18–65 whose radiographs were available.
- Radiographs that included the entire imaging area of both temporal bones and semicircular canals in the inner ear.

Exclusion criteria

- Low-quality images with noise and scatter.
- Images where the desired areas are not within the imaging area, or where there are errors due to the patient or device during imaging.
- Radiographs with interrupted bone margins.
- Patients who have had tumor formation or surgical operations in the areas to be examined due to trauma or accident in the head and neck region.

Imaging method

All patients underwent axial CT scan (tube voltage, kV 120; 200–300 mA; field of view, 25 cm; high resolution, 0.6 mm contiguous axial slice) obtained using a SIEMENS SOMATOM DEFINITION AS + 128-Detector Spiral MSCT device. Measurements were performed from the obtained images using the RadiAnt program. For power analysis of the parameters, effect size and α: 0.05 and β: 0.95, were taken, and calculations were made using the G power 3.1 statistical analysis program, and d: 0.49 was found. All the measurements were made by semi-automatically determined using thresholds. All measurements were made by a radiologist and a clinical anatomist at different times and independently of each other. The study examined intra-observer and inter-observer agreement by calculating Cohen's kappa coefficient and intra-class correlation coefficient. Inter-observer agreement was analyzed as 95% (Figs. 1, 2).

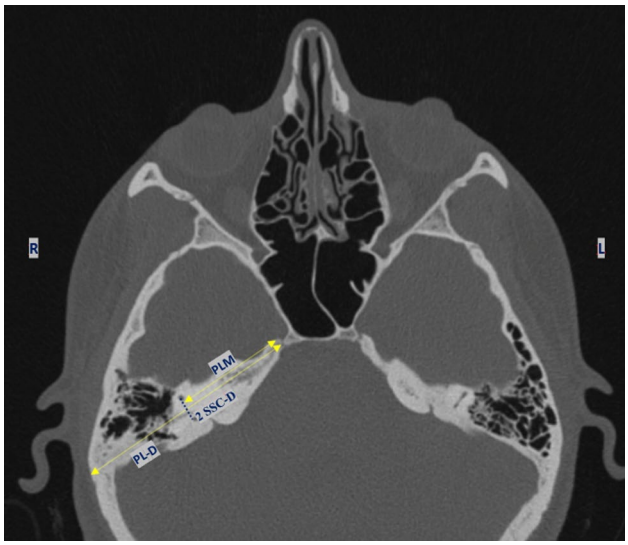

Fig. 1 CT scan of the cranium. *2 SSC-D* The distance between the two arms of the superior semicircular canal, *PLM* Length of the petrous part of the temporal bone medial to the anterior semicircular canal measured from the apex to the SSCD. The measurement was perpendicular to anterior semicircular canal diameter, *PL-D* Length of the petrous part of the TB measured from the apex to the external table of the temporal bone. The measurement was perpendicular to anterior semicircular canal diameter

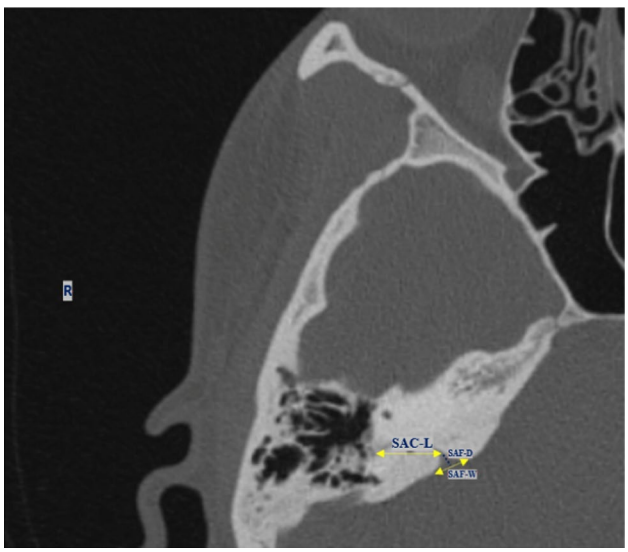

Fig. 2 CT Scan of the right side of the cranium. *SAC-L* Length of the subarcuate canal, *SAF-W* Width of subarcuate fossa, *SAF-D* Depth of subarcuate fossa

Radiological evaluation parameters

SAC-CW: The width of the cranial opening of the subarcuate canal

SAC-LW: Width of the labyrinth opening of the subarcuate canal. The width of the channel where it opens to the air cells in the axial section where it is best seen

SAC-L: Length of the subarcuate canal. A straight line was drawed connecting each end (Fig. 4)

SAF-W: Width of subarcuate fossa

SAF-D: Depth of subarcuate fossa

SSC–SAC/C: The distance of the cranial opening of the subarcuate canal to the superior semicircular canal. In Axial CT, the distance from the posterior leg of the semicircular canal to the SAC/C, SAC/L and SAC/D points in the axial section, where the canal is best seen

SSC–SAC/L: The distance of the labyrinth opening of the subarcuate canal to the superior semicircular canal

SSC–SAC/D: The closest distance of the subarcuate canal to the superior semicircular canal

2 SSC-D: The distance between the two arms of the superior semicircular canal

PLM: Length of the petrous part of the temporal bone to the anterior semicircular canal measured from the apex to the SSCD. The measurement was perpendicular to anterior semicircular canal diameter

PL-D: Length of the petrous part of the TB measured from the apex to the external table of the temporal bone. The measurement was perpendicular to anterior semicircular canal diameter

SAF–IAP/D: The closest distance between the subarcuate fossa and the posterior wall of the internal acoustic meatus

SAF-A/D: The distance between the subarcuate fossa and the ampulla of SSC

Statistical analysis

The data obtained in this study were analyzed using the Statistical Package for Social Sciences (SPSS) for Windows version 22.0 program. The normal distribution of the numerical data was tested using the Shapiro–Wilk test. Parametric tests were used when the data were normally distributed and non-parametric tests were used when the data were not normally distributed. The significance level for statistical analysis was set at $p < 0.05$.

Results

SAC-CW was determined as 44 ± 0.54 mm, SAC-LW was determined as 60 ± 0.42 mm, SAC-L was determined as 8.79 ± 2.31 mm, SAF-W was determined as 5.54 ± 1.75 mm, and SAF-D was determined as 1.67 ± 0.69 mm. SSC–SAC/C was measured as 5.33 ± 1.81 mm, SSC–SAC/L was measured as 3,90 ± ,98 mm, PLM was measured as 33.56 ± 0.42 mm, and PL was measured as 66.69 ± 0.41 mm. No statistically significant differences were found between the right and left sides (Table 1).

Table 1 Values of radiological parameters of SAC and SAF between parties

	Total	Right	Left	*p*
SAC-CW	0.44 ± 0.54	0.43 ± 0.25	0.46 ± 0.72	0.981
SAC-LW	0.60 ± 0.42	0.64 ± 1.04	0.66 ± 0.48	0.564
SAC-L	8.79 ± 2.31	8.44 ± 2.08	9.15 ± 2.47	0.230
SAF-W	5.54 ± 1.75	5.52 ± 1.79	5.57 ± 1.71	0.564
SAF-D	1.67 ± 0.69	1.64 ± 0.58	1.71 ± 0.78	1.01
SSC–SAC/C	5.33 ± 1.81	5.03 ± 1.65	5.63 ± 1.91	0.991
SSC–SAC/L	3.90 ± 0.98	3.77 ± 1.02	4.03 ± 0.92	0.095
SSC–SAC/D	1.80 ± 0.61	1.84 ± 0.68	1.76 ± 0.53	0.301
2 SSC-D	6.73 ± 0.69	6.78 ± 0.67	6.69 ± 0.71	0.271
PLM	33.56 ± 0.42	33.5 ± 0.30	33.4 ± 0.51	1.49
PL-D	66.69 ± 0.41	67.0 ± 0.44	66.1 ± 0.38	0.084
SAF–IAP/D	9.62 ± 2.4	12.18 ± 4.90	7.07 ± 2.14	0.562
SAF-A/D	9.09 ± 2.11	8.82 ± 1.96	9.37 ± 2.22	0.341

Test: Independent *t* test, $p < 0.05$ *SAC-CW* The width of the cranial opening of the subarcuate canal, *SAC-LW* Width of the labyrinth opening of the subarcuate canal, *SAC-L* Length of the subarcuate canal, *SAF-W* Width of subarquat fossa, *SAF-D* Depth of subarquat fossa, *SSC–SAC/C* The distance of the cranial opening of the subarcuate canal to the superior semicircular canal, *SSC–SAC/L* The distance of the labyrinth opening of the subarcuate canal to the superior semicircular canal, *SSC–SAC/D* The closest distance of the subarcuate canal to the superior semicircular canal, *2 SSC-D* The distance between the two arms of the superior semicircular canal, *PLM* Length of the petrous part of the temporal bone medial to the anterior semicircular canal measured from the apex to the SSCD. The measurement was perpendicular to anterior semicircular canal diameter, *PL-D* Length of the petrous part of the TB measured from the apex to the external table of the temporal bone. The measurement was perpendicular to anterior semicircular canal diameter, *SAF–IAP/D* The closest distance between the subarcuate fossa and the posterior wall of the internal acoustic meatus, *SAF-A/D* The distance between the subarcuate fossa and the ampulla

The morphological distribution of the SAC and SAF dimensions is shown in Fig. 3, along with the Gaussian curve. The study found that the SAC length was concentrated around 10 mm, while the SAC–labyrinthine width ranged from 0.04 to 1.00 mm and the SAC–cranial width ranged from 0.01 to 0.05 mm. The SAF depth was concentrated between 1.00 and 2.00 mm, and the width ranged from 4.00 to 6.00 mm.

Table 2 presents the SAC and SAF measurements according to gender. There was no difference in SAC and SAF dimensions between males and females, except for SSC–SAC/D, 2 SSC-D, PLM, and PL distances, which were longer in males than females ($p < 0.05$).

All parameters in this study were evaluated according to age. In the study, without distinguishing between the right and left sides, 60 patients under 40 years and 58 patients over

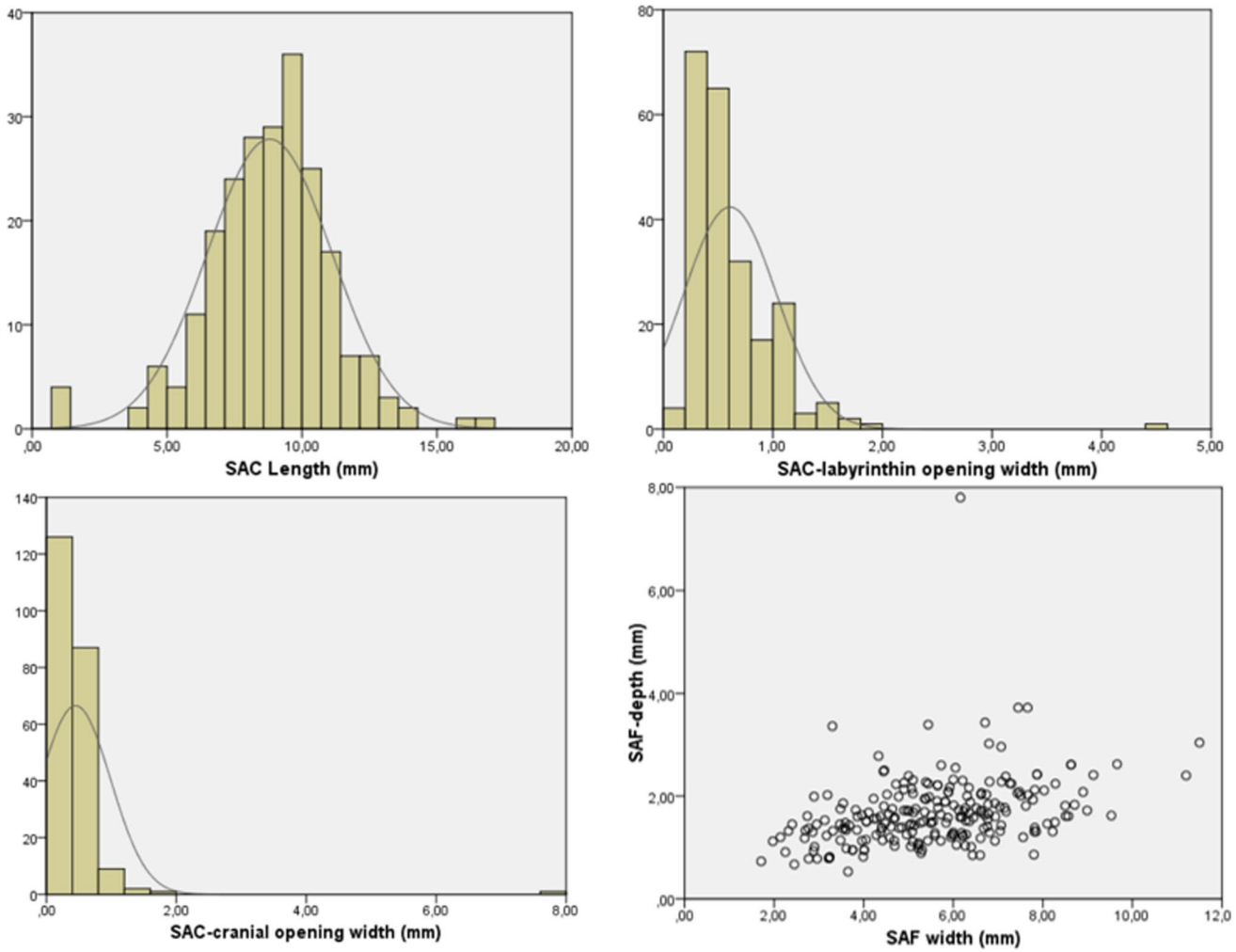

Fig. 3 Morphological distribution of SAC and SAF dimensions. The black line shows the Gaussian curve with respect to the standard deviation

40 years were analyzed separately. Only the depth and width of the SAF showed statistical significance in the measurements, with the SAF being deeper in patients over 40 years and wider in patients under 40 years ($p < 0.05$) (Fig. 4).

Discussion

Studies related to the subarcuate canal and fossa, located in the temporal bone, have mainly focused on parameters, such as the presence, visualization, and diameter of the canal [3, 10, 17, 22]. In this study, various measurements were performed to determine the important anatomical relationships between SAC and SAF in addition to the related parameters. Information about the fine structures of the temporal bone, such as the subarcuate canal and cochlear aqueduct, is necessary for proper planning of IAM tumor and cerebellopontine angle surgery, and also cochlear implant surgery, in terms of prevention of surgical complications, and prediction of the outcome of the procedure [17]. Evaluating the position of the subarcuate canal according to the guiding points before surgery can help prevent accidental injury to the SAA and ensure orientation during the procedure. The subarcuate canal serves as an anatomical landmark for surgical interventions, because it can provide a route for infections that spread from the mastoid cells to the dura and intracranial space. Therefore, knowing the course of the subarcuate canal is important for interpreting CT images of the temporal bone in patients who have suffered trauma, as misinterpretation of this structure as a fracture line can lead to an incorrect diagnosis. In addition, the clinical significance of the subarcuate canal in the development of cerebrospinal fluid fistulas and the spread of infections facilitates diagnosis [3]. This study was conducted to highlight the clinical importance of the relevant regional anatomy by focusing on the morphology of the SAC and SAF.

Similar to the study conducted by Tekdemir et al. [6], our study found that the subarcuate canal progressed as a

Table 2 Evaluation by gender

	Female	Male	*p*
SAC-CW	0.41 ± .23	0.48 ± .73	0.291
SAC-LW	0.60 ± .35	0.60 ± .49	0.970
SAC-L	8.86 ± 2.28	8.72 ± 2.35	0.647
SAF-W	5.89 ± 1.91	5.70 ± 1.57	0.176
SAF-D	1.60 ± .58	1.75 ± .78	0.095
SSC–SAC/C	5.49 ± 1.80	5.16 ± 1.81	0.177
SSC–SAC/L	3.83 ± .99	3.97 ± .97	0.287
SSC–SAC/D	1.70 ± .47	1.90 ± .72	**0.017**
2 SSC-D	66.21 ± 6.89	68.53 ± 6.79	**0.011**
PLM	32.87 ± 4.56	34.18 ± 3.97	**0.020**
PL-D	6.55 ± .34	6.97 ± .45	**0.000**
SAF–IAP/D	11.92 ± 3.45	7.28 ± 2.13	0.317
SAF-A/D	9.32 ± 2.31	8.86 ± 1.87	0.721

Test: independent t test, p < 0.05 SAC-CW The width of the cranial opening of the subarcuate canal, *SAC-LW* Width of the labyrinth opening of the subarcuate canal, *SAC-L* Length of the subarcuate canal, *SAF-W* Width of subarquat fossa, *SAF-D* Depth of subarquat fossa, *SSC–SAC/C* The distance of the cranial opening of the subarcuate canal to the superior semicircular canal, *SSC–SAC/L* The distance of the labyrinth opening of the subarcuate canal to the superior semicircular canal, *SSC–SAC/D* The closest distance of the subarcuate canal to the superior semicircular canal, *2 SSC-D* The distance between the two arms of the superior semicircular canal, *PLM* Length of the petrous part of the temporal bone medial to the anterior semicircular canal measured from the apex to the SSCD. The measurement was perpendicular to anterior semicircular canal diameter, *PL-D* Length of the petrous part of the TB measured from the apex to the external table of the temporal bone. The measurement was perpendicular to anterior semicircular canal diameter, *SAF–IAP/D* The closest distance between the subarcuate fossa and the posterior wall of the internal acoustic meatus, *SAF-A/D* The distance between the subarcuate fossa and the ampulla

single canal and was closer to the non-ampullated end of the superior semicircular canal. This course can be a criterion for surgeons performing surgical interventions in the inner ear. The period between birth and 5 years of age is the period when the petrous part of the temporal bone develops the most intensely in individuals younger than 5 years. During the period from birth to 5 years of age, the SAF undergoes a transformation towards the SAC [11]. Although relatively large after birth, the SAF gradually decreases in size [23]. The morphology of the SAF starts to resemble that of adults in the fifth year of life, with the SAF narrowing towards the canal [5]. Migirov and Kronenberg supported Proctor's findings and reported no significant differences in SAF morphology between larger children and adults [5, 17]. We conducted our study on adult individuals and found that the SAF was deeper in patients over 40 years, while it was wider in patients under 40 years. Studies measuring the depth and width of the SAF cannot be found in literature. In our study, when these parameters were evaluated, the width of the SAF was found to be 5.55 ± 1.75 mm and the depth was 1.67 ± 0.69 mm.

Wilbrand et al. reported that the length and width of the SAC, especially in the area of the perilabyrinth, were influenced by the degree of pneumatization and size of the temporal bone, and in their study, they noted that the diameter of this canal reached between 0.5 and 1 mm until adulthood [9]. Krombach et al. defined the mean diameter of the SAC with an absolute value of 0.5 ± 0.2 mm in a study of 20 petrous bone CT scans from 10 males and 10 females with an average age of 42 years [3]. In another study, the average diameter of the SAC was calculated to be 1.16 ± 0.4 mm in a CT study of 316 petrous bones with an average age of 53.3 [8]. Tekdemir et al. found in an anatomical microdissection study on 12 cadavers and 35 dry temporal bones that the mean width of the SAC was approximately 1 mm [6].

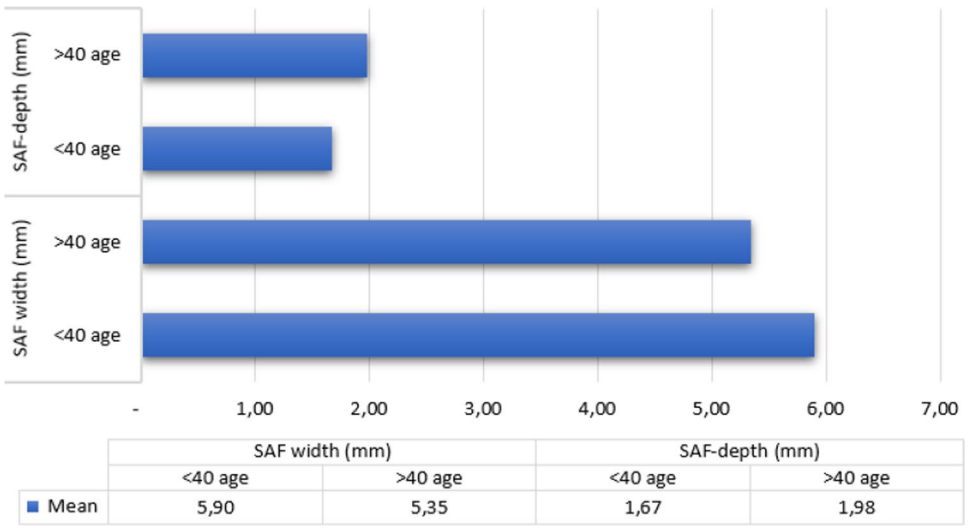

Fig. 4 Variation of SAF depth and width with age

In Kenis et al.'s study, the width of the SAC was found to be 0.69 mm in children over 6 years [24]. In our study, we measured not the mean diameter of the canal, but the width of the medial opening facing the subarcuate fossa (SAF) and the lateral opening facing the mastoid antrum. The lateral opening of the SAC was found to be 0.44 ± 0.54 mm and the medial opening was 0.60 ± 0.42 mm. Considering that the diameter of the canal does not show significant changes throughout its course, these values support those reported in the literature.

SAC has been described as a canal that passes between the two limbs of the SSC and over the lateral semicircular canal [3, 5]. Trauma to this structure can lead to bleeding or cerebrospinal fluid leakage, and in rare cases, facial nerve injury [5]. Therefore, it is important for surgeons to determine the location of the SAF on petrous CT imaging. Middle ear infections or chronic middle ear diseases can also lead to meningitis through the canal [8]. Therefore, it is important to evaluate the dimensions and location of SAC in relation to adjacent structures. To examine the relationship between the SAC and the SSC, three measurements were taken from the posteromedial limb of the SSC to the medial opening of the SAC, the lateral opening of the SAC, and the closest distance to the SAC from the posteromedial limb of the SSC. These values were found to be 3.90 ± 0.98 mm, 5.33 ± 1.81 mm, and 1.80 ± 0.61 mm, respectively. In addition, the distance from the ampulla, where the anterior and lateral semicircular canals meet, to the medial opening of the SAC was measured in this study, and this value was calculated as 9.09 ± 2.11 mm.

After birth, the petrous portion of the temporal bone rapidly grows along the longitudinal axis, especially during the first 2 years of life [25, 26]. The petrous portion of the temporal bone is characterized by a complex growth pattern [25, 27]. In Maslanka et al.'s study on the temporal bone of children aged 0–5 years, both PL and PLM increased continuously with age. During the 60-month period studied, the length of the pyramid varied between 35.1 mm and 63.9 mm, and the PLM distance increased from 16.5 to 32.3 mm [11]. In addition, SSCD did not correlate with age, and its value was more constant between age groups, ranging from 6.7 to 10.5 mm [11]. In our study, the PL value of individuals aged 18–65 years was found to be an average of 66.69 ± 0.41 mm, and the PLM value was an average of 33.56 ± 0.42 mm. Maslanka et al.'s samples show that the PM and PLM values of 5-year-old children are very close to those of adult individuals. From this, it can be concluded that the development of the temporal bone continues until the age of 5 and that the dimensions reach adult values in adulthood. In addition, when evaluating the SSCD value, which is the outer diameter of the SSC lumen measured between the most distal points, it was found to be an average of 6.73 ± 0.69 mm in our study. The value we obtained supports Maslanka et al.'s conclusion that SSCD does not correlate with age, and is consistent with our measurement results.

Typically, the SCA is completely surrounded by compact bone. As a variant of individuals with strong pneumatization of the temporal bone, a canal can be seen surrounded by thin compact bone that moves between the mastoid cells. In such cases, it can be shortened due to expansion of the mastoid cells after a shorter passage from the temporal bone [3]. In a study by Steinbach et al. on adult individuals' temporal bones, the length of the SAC was found to be 10.7 ± 0.9 mm (the lowest value being 4.25 mm, and the highest value being 16.1 mm [8]. In a study on cadavers aged between 52 and 64, the length of the SAC was found to be an average of 9.2 mm (6). In our study, the SAC length was determined to be 8.79 ± 2.31 mm. The different values found in these studies may be a possible result of pneumatization of the temporal bone or the type of sample.

During any surgical intervention on the posterior petrous bone for the removal of acoustic tumors, damage to the SAA may occur, because acoustic tumors generally extend beyond the IAM [5]. During the excision of intracanalicular acoustic neuromas, it is especially important to ensure this anatomical orientation when circumventing the posterior wall of the IAM using the retrosigmoid approach. Migirov et al. identified a SAC originating from the internal acoustic canal in four of their 488 CT images (0.8%). In Wilbrand et al.'s study, the SAC started from the IAM in 16 out of 61 cadavers [9]. Based on this information, in our study, when the medial opening of the SAC started from the SAF, the distance between the deepest point of the SAF and the posterior edge of the IAM was measured to be 9.62 ± 2.4 mm. In a study on dry skulls by Tekdemir et al., this distance was reported to be an average of 4.2 mm [6]. We believe that the difference between these two measurements is due to methodological differences and the fact that the IAM and SAF do not lie in the same plane.

Conclusion

The morphometric measurements obtained in this study can provide useful information for neurosurgeons, neurotologist and otolaryngologists involved in retrosigmoid approach for internal acoustic meatus tumor surgery and cerebellopontine angle surgery, and for patients undergoing cochlear implant planning with a retrofacial approach in terms of prevention of surgical complications, the prediction of the outcome of the procedure. In addition, it is important to know the location of the SAC on petrous CT imaging to avoid confusion with a possible fracture line, and surgical studies are recommended in this regard.

Author contributions AD: writing—review and editing, resources, formal analysis, data collection, project development, manuscript editing. AHM: writing—original draft, methodology, investigation, data management, data analysis, manuscript writing. TDB: writing—original draft, methodology, investigation, supervision, project development, data analysis, manuscript editing. KA: writing—review and editing, resources, formal analysis, data collection. ÇF: writing—review, resources formal analysis, data collection, manuscript editing. PD: writing—original draft, methodology, investigation, data management, data analysis, manuscript writing. BB: writing—review and editing, resources, formal analysis, supervision, manuscript editing.

Funding The authors declare that no funds, grants, or other support were received during the preparation of this manuscript.

Data availability The data that support the findings of this study are available on request from the corresponding author. The data are not publicly available due to privacy or ethical restrictions.

Declarations

Conflict of interest The authors declare that there is no conflict of interest.

Ethics approval This study was performed in line with the principles of the Declaration of Helsinki. Approval was obtained from the Private Bayındır Hospital Söğütözü Ethics Committee. (Date 25.04.2023/No 11/23).

References

1. Ding AS, Lu A, Li Z, Galaiya D, Siewerdsen JH, Taylor RH, Creighton FX (2022) Automated registration-based temporal bone computed tomography segmentation for applications in neurotologic surgery. Otolaryngol Head Neck Surg 167(1):133–140
2. Wadin K, Wilbrand H (1986) The topographic relations of the high jugular fossa to the inner ear: a radioanatomic investigation. Acta Radiol Diagn (Stockh). 27:315–324
3. Krombach G, Schmitz-Rode T, Prescher A (2002) The petromastoid canal on computed tomography. Eur Radiol 12:2770–2775
4. Skrzat J, Leszczyński B, Kozerska M, Wróbel A (2013) Topography and morphometry of the subarcuate canal. Folia Morphol (Warsz). 72(4):357–361
5. Proctor B (1983) The petromastoid canal. Ann Otol Rhinol Laryngol 92:640–644
6. Tekdemir I, Aslan A, Elhan A (1999) The Subarcuate canaliculus and its artery—a radioanatomical study. Ann Anatomy-Anatomischer Anzeiger. 181:207–211
7. Standring S (2005) Gray's anatomy, 39th edn. Elseiver, London
8. Steinbach S, Fitzthum A, Reiser M et al (2009) The petromastoid canal: a computed tomography investigation. HNO 57:142–145
9. Wilbrand H, Rauschning W, Ruhn G (1986) The Subarcuate fossa and channel: a radioanatomic investigation. Acta Radiol Diagn (Stockh). 27:637–644
10. Migirov L, Kronenberg J (2006) Radiology of the petromastoid canal. Otol Neurotol 27:410–413
11. Maślanka M, Skadorwa T, Ciszek B (2018) Postnatal development of the Subarcuate fossa and Subarcuate canaliculus—a computed tomographic study. Surg Radiol Anat 40:1111–1117
12. Büyüktepe M, Doğan İ (2020) Suboksipital Orta Hat ve Retrosigmoid Yaklaşımda Anatomik Temeller. Türk Nöroşirürji Derg. 30:165–171
13. Baskaya MK, Pyle GM, Roche JP et al (2019) Retrosigmoid approach for vestibular schwannoma surgery. Vestibular Schwannoma Surg. 89:105–133
14. Grammatica A, Alicandri-Ciufelli M, Molteni G et al (2010) Subarcuate canal and artery: a case report. Surg Radiol Anat 32:171–174
15. Akyol Y, Galheigo D, Massimore M et al (2011) Subarcuate artery and canal: an important anatomic variant. J Comput Assist Tomogr 35:688–689
16. Cömert E, Cömert A, Çay N et al (2014) Surgical anatomy of the infralabyrinthine approach. Otolaryngol-Head Neck Surg. 151:301–307
17. Migirov L, Kronenberg J (2009) Petromastoid canal and cochlear aqueduct in cochlear implant candidates. Otolaryngol—Head Neck Surg 140:419–422.
18. Rhoton AL Jr (1993) Microsurgical anatomy of posterior fossa cranial nerves. Surgery Cranial Nerves Posterior Fossa. 23:1–103
19. Chouhan M, Kumbhat P (2022) Anomalous subarcuate canal and artery: a rare anatomical variation. Iran J Otorhinolaryngol. 34:187
20. de Abreu CEC, Cruz OLM (2007) Surgical anatomy of anterior and retrofacial approaches to sinus tympani. Otol Neurotol 28:682–684
21. Yilmazer R, Gerring RC, Sidani C et al (2018) The feasibility of retrofacial approach for cochlear implantation. Otol Neurotol 39:550-e556
22. Koral K, Vachha B, Gimi B et al (2014) MRI of the petromastoid canal in children. J Magn Reson Imaging 39:966–971
23. Gannon PJ, Eden AR, Laitman JT (1988) The Subarcuate fossa and cerebellum of extant primates: comparative study of a skull-brain interface. Am J Phys Anthropol 77:143–164
24. Kenis C, Ditchfield M, Paul E et al (2013) The petromastoid canal in the young child: appearance on computed tomography. Int J Pediatr Otorhinolaryngol 77:803–807
25. Hilding DA (1987) Petrous apex and Subarcuate fossa maturation. Laryngoscope 97:1129–1135
26. Eby TL, Nadol JB Jr (1986) Postnatal growth of the human temporal bone: implications for cochlear implants in children. Ann Otol Rhinol Laryngol 95:356–364
27. Skadorwa T, Maślanka M, Ciszek B (2015) The morphology and morphometry of the fetal fallopian canal: a microtomographic study. Surg Radiol Anat 37:677–684